

# Interenzyme Substrate Diffusion for an Enzyme Cascade Organized on Spatially Addressable DNA Nanostructures

Jinglin Fu,<sup>†,‡,⊥</sup> Minghui Liu,<sup>†,§,⊥</sup> Yan Liu,<sup>†,§</sup> Neal W. Woodbury,<sup>\*,‡,§</sup> and Hao Yan<sup>\*,†,§</sup>

<sup>†</sup>Center for Single Molecule Biophysics, <sup>‡</sup>Center for Innovations in Medicine, The Biodesign Institute, <sup>§</sup>Department of Chemistry and Biochemistry, Arizona State University, Tempe, Arizona 85287, United States

**S** Supporting Information

**ABSTRACT:** Spatially addressable DNA nanostructures facilitate the self-assembly of heterogeneous elements with precisely controlled patterns. Here we organized discrete glucose oxidase (GOx)/horseradish peroxidase (HRP) enzyme pairs on specific DNA origami tiles with controlled interenzyme spacing and position. The distance between enzymes was systematically varied from 10 to 65 nm, and the corresponding activities were evaluated. The study revealed two different distance-dependent kinetic processes associated with the assembled enzyme pairs. Strongly enhanced activity was observed for those assemblies in which the enzymes were closely spaced, while the activity dropped dramatically for enzymes as little as 20 nm apart. Increasing the spacing further resulted in a much weaker distance dependence. Combined with diffusion modeling, the results suggest that Brownian diffusion of intermediates in solution governed the variations in activity for more distant enzyme pairs, while dimensionally limited diffusion of intermediates across connected protein surfaces contributed to the enhancement in activity for closely spaced GOx/HRP assemblies. To further test the role of limited dimensional diffusion along protein surfaces, a noncatalytic protein bridge was inserted between GOx and HRP to connect their hydration shells. This resulted in substantially enhanced activity of the enzyme pair.

Cellular activities are directed by complex, multienzyme synthetic pathways that exhibit extraordinary yield and specificity. Many of these enzyme systems are spatially organized to facilitate efficient diffusion of intermediates from one protein to another by substrate channeling<sup>1,2</sup> and enzyme encapsulation.<sup>3</sup> Understanding the effect of spatial organization on enzymatic activity in multienzyme systems is not only fundamentally interesting, but also important for translating biochemical pathways to noncellular environments. Despite the importance, there are very few methods available to systematically evaluate how spatial factors (e.g., position, orientation, enzyme ratio) influence enzymatic activity in multienzyme systems.

DNA nanotechnology has emerged as a reliable way to organize nanoscale systems because of the programmability of DNA hybridization and versatility of DNA-biomolecule conjugation strategies.<sup>4</sup> The *in vitro* and *in vivo* assembly of several enzymatic networks organized on two-dimensional

DNA and RNA arrays<sup>5</sup> or simple DNA double helices<sup>6</sup> has led to the enhancement of catalytic activities. Nevertheless, the nucleic acid scaffolds used in these studies are limited in their ability to study spatial parameters in multienzyme systems because of the lack of structural complexity. The development of the DNA origami method<sup>7</sup> provides an addressable platform upon which to display nucleic acids or other ligands, permitting the precise patterning of multiple proteins or other elements.<sup>8</sup> Here, we report a study of the distance-dependence for the activity of glucose oxidase (GOx)/horseradish peroxidase (HRP) cascade by assembling a single GOx/HRP pair on a discrete, rectangular DNA origami tile.

The DNA-directed coassembly of GOx and HRP on DNA origami tiles is illustrated in Figure 1A. The DNA-conjugated

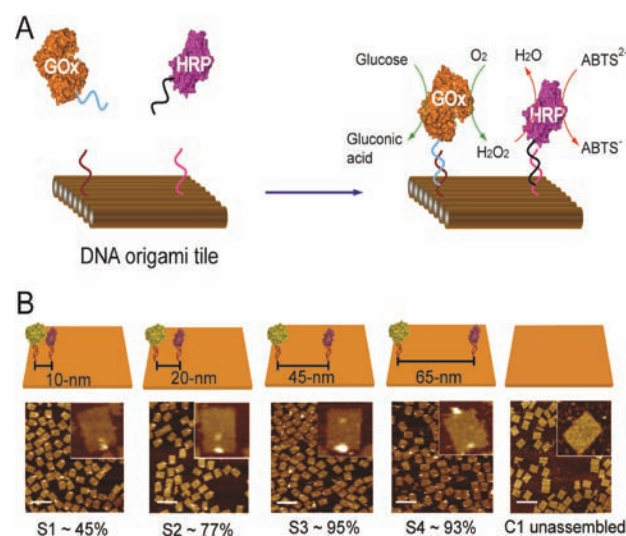


**Figure 1.** DNA nanostructure-directed coassembly of GOx and HRP enzymes with control over interenzyme distances. (A) The assembly strategy and details of the GOx/HRP enzyme cascade. (B) Rectangular DNA origami tiles with assembled GOx/HRP pairs spacing from 10 to 65 nm. GOx/HRP coassembly yields were determined from AFM images as shown in the bottom panel. Scale bar: 200 nm.

enzymes, GOx-poly(T)<sub>22</sub> (5'-HS-TTTTTTTTTTTTTTTT TTTT TT-3') and HRP-poly(GGT)<sub>6</sub> (5'-HS-TTGGTGGTGGTGGTGGTGGT-3'), were assembled on

Received: January 27, 2012

Published: March 13, 2012

rectangular DNA origami tiles ( $\sim 60 \times 80$  nm) by hybridizing with the corresponding complementary strands displayed on the surface of the origami scaffolds. Four different rectangular origami tiles<sup>9</sup> were prepared with interenzyme probe distances (distance between two protein-binding sites) of 10 nm (S1), 20 nm (S2), 45 nm (S3), and 65 nm (S4). For detailed sample preparations, please see Figures S1–S6 (Supporting Information (SI)). To achieve high coassembly yields of the GOx/HRP pairs, a 3-fold excess of enzymes were incubated with the DNA tiles (Figure S7 (SI)). The coassembly of the GOx/HRP cascade was visualized using AFM imaging of DNA nanostructures. The presence of a protein results in a higher region than the surrounding surface of the origami tile (Figures S8–9, S16–17 (SI)). Most origami tiles were deposited on the mica surface with the protein decorated side facing up, likely because of the strong interaction (charge or stacking) of the opposite flat side with the mica surface.

As shown in Figure 1B, high coassembly yields of GOx/HRP pairs on DNA origami tiles were achieved for longer interenzyme distances, with  $\sim 95\%$  for S3 (45 nm) and  $\sim 93\%$  for S4 (65 nm). For shorter distances, the coassembly of GOx/HRP pairs was less efficient because of the steric hindrance between two nearby enzymes, with  $\sim 45\%$  for S1 (10 nm) and  $\sim 77\%$  for S2 (20 nm). To rule out any nonspecific absorption of the enzymes to the tile surfaces, a control experiment was performed where tiles without any nucleic acid probes (C1) were incubated with DNA modified GOx and HRP, and no binding of the enzymes to the tiles was observed. The activities of the enzyme complexes, containing all components of GOx/HRP coassembled on DNA tiles, unbound enzymes and free DNA tiles were measured in the presence of substrates glucose and ABTS<sup>2-</sup> by monitoring the increase in absorbance at 410 nm (Figure 2A). The S1 (10 nm) tile solution exhibited the highest enzyme activity, which was more than 2 times greater than the activity of the S2 (20 nm) tile solution (Figure 2B), even though the coassembly yield of GOx/HRP pairs was significantly lower for S1 tiles. Increasing the distance between GOx and HRP from 20 to 65 nm resulted in a small decrease in the raw enzyme activity ( $\sim 10\%$ ). A similar distance-dependent trend in activity was also observed in additional interenzyme distance-dependence studies using a different attachment scheme (Figure S10 (SI)). All samples containing assembled GOx/HRP tiles exhibited higher activities than unassembled enzyme controls, demonstrating how arranging the enzymes in close proximity results in enhanced activity. Further, the control solutions (with free enzymes and unbound DNA tiles) had similar activities as free enzymes without any DNA nanostructures, confirming that a DNA-nanostructure environment does not affect enzyme activity under the conditions used.

$$A_{\text{raw}} = \frac{Y_{\text{assem}}}{3} A_{\text{assem}} + \frac{3 - Y_{\text{assem}}}{3} A_{\text{unassem}} \quad (1)$$

Equation 1 was used to adjust the activities to account for the differences in yields of coassembled enzymes. In eq 1, the raw activity ( $A_{\text{raw}}$ ) consists of contributions from both assembled GOx/HRP cascades ( $A_{\text{assem}}$ ) and unassembled enzyme ( $A_{\text{unassem}}$ ), where  $Y_{\text{assem}}$  is the coassembly yield of GOx/HRP pairs on the origami tiles. Because a 3:1 ratio of enzymes to origami tiles was used for the assembly, the percentage of assembled enzymes was  $\sim (Y_{\text{assem}}/3)$ , while the percentage of unassembled enzymes was  $\sim ((3 - Y_{\text{assem}})/3)$ . The resulting calibrated activities are presented in Figure 2B. The largest enhancement in activity was observed for enzymes with 10 nm

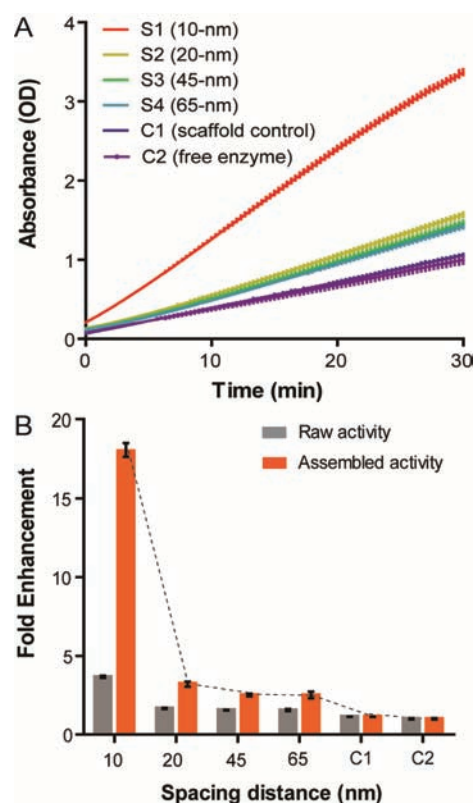


**Figure 2.** Spacing distance-dependent effect of assembled GOx/HRP pairs as illustrated by (A) plots of product concentration vs time for various nanostructured and free enzyme samples and (B) enhancement of the activity of the enzyme pairs on DNA nanostructures compared to free enzyme in solution. Both the raw activity (uncorrected for the yield of the completely assembled nanostructures) and yield-corrected activity are shown. The activity correction for assembly yields was performed using eq 1.

spacing, which was more than 15 times higher than the corresponding control. A sharp decrease in cascade activity occurred as the interenzyme distance was increased from 10 to 20 nm, followed by a slow and gradual decrease in activity as the distance was further increased to 65 nm.

For a GOx/HRP cascade, effective transfer of the intermediate  $\text{H}_2\text{O}_2$  between the enzymes is essential to the cascade activity (Figure 3A). Here, we use Brownian motion to simulate the distance-dependent, three-dimensional (3D) diffusion of  $\text{H}_2\text{O}_2$  between enzymes as described by eq 2, where  $n(r,t)$  is the concentration of  $\text{H}_2\text{O}_2$  at a distance  $r$  from the initial position,  $D$  is the diffusion coefficient, and  $t$  is the diffusion time.<sup>10</sup> GOx is assumed to generate  $\text{H}_2\text{O}_2$  at a constant rate,  $k_{\text{cat}}$ . Equation 3 describes the convolution function of Brownian motion of  $\text{H}_2\text{O}_2$  with a constant catalytic rate for a GOx/HRP pair in the given time  $t$ , where  $\tau$  is the average time between GOx turnovers ( $1/k_{\text{cat}}$ ). Figure 3B shows the simulation result using the following parameters:  $D = 1000 \mu\text{m}^2/\text{s}$  for  $\text{H}_2\text{O}_2$ ,<sup>11</sup>  $k_{\text{cat}} = 300 \text{ s}^{-1}$  for GOx (Figure S11 (SI)), and  $t = 1 \text{ s}$ . Because of the rapid diffusion of  $\text{H}_2\text{O}_2$  in water, the concentration of  $\text{H}_2\text{O}_2$  drops off only slightly within a few hundred nanometers of GOx. If one assumes that the activity is linear with substrate concentration, this simulation result agrees with the observation that assembled GOx/HRP cascades exhibit only small variations in activity for interenzyme distances between 20 and 65 nm. For a 1 nM solution of unassembled enzymes, the average spacing between proteins is

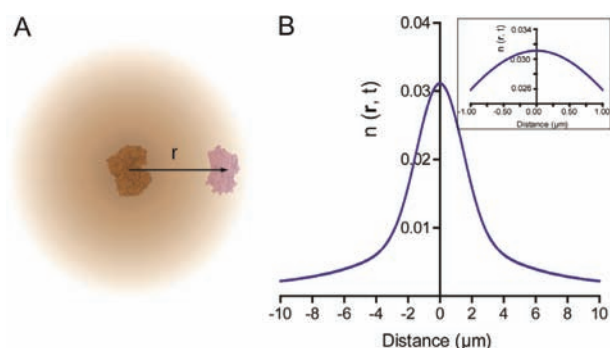


**Figure 3.** Model of  $\text{H}_2\text{O}_2$  diffusion in a single GOx/HRP pair. (A) Simplified illustration of the distance-dependent ( $r$ )  $\text{H}_2\text{O}_2$  concentration gradient resulting from 3D Brownian diffusion. (B) Simulated  $\text{H}_2\text{O}_2$  concentration gradient as a function of distance between GOx and HRP using eq 3 with the following parameters: diffusion coefficient  $\sim 1000 \mu\text{m}^2/\text{s}$ ;  $k_{\text{cat}}$  (GOx)  $\sim 300 \text{ s}^{-1}$ ; and the integration time  $\sim 1 \text{ s}$ . Inset shows the enlarged distance-dependent  $\text{H}_2\text{O}_2$  concentration gradient within  $1 \mu\text{m}$ .

$\sim 1.2 \mu\text{m}$ , where the  $\text{H}_2\text{O}_2$  concentration is  $\sim 60\%$  of the initial position in the simulation. This result is consistent with the limited activity enhancement (less than 2-fold) for distantly spaced GOx/HRP pairs (e.g., 45 or 65 nm) compared to unassembled enzymes in Figure 2. Further, if the intermediate transfer between distantly spaced enzymes is dominated by Brownian motion, diluting the sample will result in a decreased  $\text{H}_2\text{O}_2$  concentration for free HRP, while the  $\text{H}_2\text{O}_2$  concentration near HRP in the assembled complexes remains nearly constant. Thus greater activity enhancement will be observed for assembled GOx/HRP pairs relative to the free enzymes under these conditions. This concentration-dependent enhancement was confirmed by performing the assay at a range of GOx/HRP concentrations (Figure S12 (SI)).

$$n(r, t) = \frac{1}{(4\pi Dt)^{3/2}} \exp\left(-\frac{r^2}{4Dt}\right) \quad (2)$$

$$n(r, t) = \sum_{i=0}^{i=t/\tau-1} \frac{1}{(4\pi D(t-i\tau))^{3/2}} \exp\left(-\frac{r^2}{4D(t-i\tau)}\right) \quad (3)$$

While the Brownian diffusion model is consistent with the interenzyme distance dependence of the activity at distances greater than 20 nm, the strong activity enhancement for GOx/HRP pairs spaced 10 nm apart cannot be explained by this model. Apparently, the transfer of  $\text{H}_2\text{O}_2$  between closely spaced enzymes is governed by a different mechanism than that for more distantly spaced enzymes. Since both GOx and HRP are randomly oriented on the DNA origami tiles, it is unlikely that the active sites of GOx and HRP are perfectly aligned to allow the direct transfer of  $\text{H}_2\text{O}_2$  between active sites. It seems more likely that when GOx and HRP are spaced in very close proximity, the two protein surfaces become essentially connected with one another, as demonstrated by AFM imaging of S1 tiles for 10 nm interenzyme spacing (Figure 1B). One possibility is that under these circumstances,  $\text{H}_2\text{O}_2$  does not generally escape into the bulk solution but instead transfers from GOx to HRP along their mutual, connected protein surface, providing a dimensionally limited diffusion mechanism that dominates over three-dimensional diffusion when the two

enzymes are essentially in contact. In support of this concept, it is known that water molecules are translationally and rotationally constrained in the hydration layer around a protein, relative to bulk solution, because of hydrogen bonding and Coulombic interactions with the protein.<sup>12</sup> Some simulation results have suggested that  $\text{H}_2\text{O}_2$  also has an affinity for protein surfaces resulting in an even longer residence time in the hydration layer near the protein than water.<sup>13</sup> In addition, dimensionally limited diffusion has been observed in a number of biochemical systems, resulting in decreased times for diffusion of a substrate or ligand to its point of action.<sup>1</sup> Examples include linear diffusion of nuclease or transcription factors along DNA<sup>14</sup> and the surface-attached “lipoyl swing arm” in the pyruvate dehydrogenase complex.<sup>2</sup>

If the enhancement seen in Figure 2 at 10 nm interenzyme distance is in fact due to dimensionally restricted diffusion along protein surfaces, it should be possible to enhance the activity observed at longer interenzyme distances by placing a protein bridge between the enzymes. To test this, we designed a ‘bridge-based’ cascade in which a noncatalytic protein was inserted between GOx and HRP, in order to connect the protein hydration shells and facilitate the surface-limit diffusion of  $\text{H}_2\text{O}_2$ . As shown in Figure 4A, a GOx/HRP pair was first assembled on a DNA origami tile with a 30 nm interenzyme distance. Next, a noncatalytic protein, either neutravidin (NTV) or streptavidin (STV)-conjugated  $\beta$ -galactosidase ( $\beta$ -Gal), was inserted between the enzymes. As shown in Figure 4B, assembled GOx/HRP pairs with a  $\beta$ -Gal bridge exhibited  $\sim 42 \pm 4\%$  higher raw activity than control assemblies without the bridge. For this preparation, the yield of assemblies with all three components (GOx, HRP, and the bridge) was  $\sim 38\%$ . Assembled GOx/HRP pairs with a NTV bridge showed  $\sim 20 \pm 4\%$  enhancement in raw activity compared to the control sample, at  $\sim 50\%$  coassembly yield (Figures S13, S18 (SI)). STV conjugated  $\beta$ -Gal and NTV in solution did not affect GOx/HRP activities (Figure S14 (SI)). With a larger protein diameter ( $\sim 16 \text{ nm}$ ),  $\beta$ -Gal can fill the space between GOx and HRP more completely than NTV ( $\sim 6 \text{ nm}$  diameter), resulting in a more enhanced activity for the  $\beta$ -Gal bridge even with a lower coassembly yield (Figure S15 (SI)). This result supports the notion that surface-limited diffusion of  $\text{H}_2\text{O}_2$  between closely spaced enzymes is responsible for the increase in cascade activity beyond what is possible by three-dimensional Brownian diffusion.

In conclusion, we have systematically studied the activity of a GOx/HRP cascade spatially organized on a DNA nanostructure as a function of interenzyme distance. The intermediate transfer of  $\text{H}_2\text{O}_2$  between enzymes was found to follow the surface-limited diffusion for closely spaced enzymes, while 3D Brownian diffusion dominated  $\text{H}_2\text{O}_2$  transfer between enzymes with larger spacing distances. These studies imply that the strong activity enhancement observed for assembled enzyme cascades is not simply achieved by reducing the interenzyme distance to reach high local molecule concentration, but also results from restricting diffusion of intermediates to a two-dimensional surface connecting the enzymes. While it is possible that some coassembled GOx/HRP pairs are aligned in such a way that their active sites are juxtaposed, facilitating  $\text{H}_2\text{O}_2$  transfer between enzyme pockets, there was no specific attempt to orient the enzymes in this study. In the future, it will be important to study the effect of enzyme orientation on the activity of assembled enzyme complexes as well.<sup>15</sup> With the further development of DNA–protein attachment chemistry



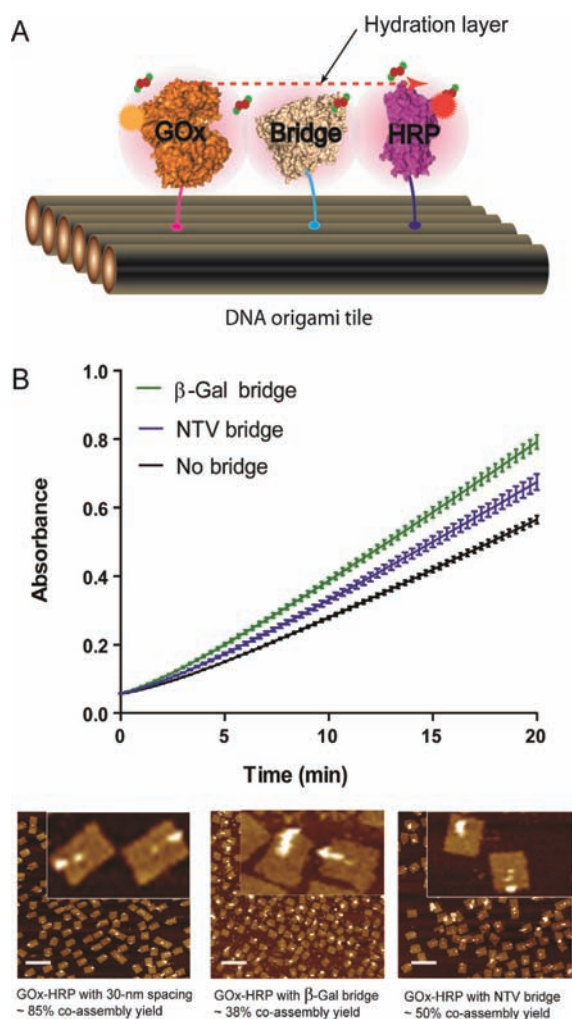


**Figure 4.** Surface-limited  $\text{H}_2\text{O}_2$  diffusion induced by a protein bridge. (A) The design of an assembled GOx/HRP pair with a protein bridge used to connect the hydration surfaces of GOx and HRP. (B) Enhancement in the activity of assembled GOx/HRP pairs with  $\beta$ -Gal and NTV bridges compared to unbridged GOx/HRP pairs. AFM images of GOx/HRP pairs with and without protein bridges were used to estimate the coassembly yield. Scale bar: 200 nm.

through site-specific conjugation or ligand capture,<sup>16</sup> it should be possible to start to direct the flow of substrate molecules between active sites using some of the concepts and tools discussed above.

## ■ ASSOCIATED CONTENT

### 📄 Supporting Information

Detailed methods and supplementary figures and tables. This information is available free of charge via the Internet at <http://pubs.acs.org/>

## ■ AUTHOR INFORMATION

### Corresponding Author

Hao.Yan@asu.edu; nwoodbury@asu.edu

### Author Contributions

<sup>†</sup>These authors contributed equally.

### Notes

The authors declare no competing financial interest.

## ■ ACKNOWLEDGMENTS

The authors acknowledge the funding support from the Army Research Office, National Science Foundation, Office of Naval Research, National Institute of Health, Department of Energy, and Sloan Foundation. The authors would like to thank Jeanette Nangreave for the help in editing the manuscript. The authors are grateful to Nils Walter, Alex Johnson-Buck, Nicole Michelotti, and Tristan Tabouillot from University of Michigan for insightful discussions and suggestions.

## ■ REFERENCES

- (1) Miles, E. W.; Rhee, S.; Davies, D. R. *J. Biol. Chem.* **1999**, *274*, 12193.
- (2) Perham, R. N. *Annu. Rev. Biochem.* **2000**, *69*, 961.
- (3) (a) Srere, P. A.; Mosbach, K. *Annu. Rev. Microbiol.* **1974**, *28*, 61. (b) Yeates, T. O.; Kerfeld, C. A.; Heinhorst, S.; Cannon, G. C.; Shively, J. M. *Nat. Rev. Microbiol.* **2008**, *6*, 681.
- (4) (a) Lin, C.; Liu, Y.; Yan, H. *Biochemistry* **2009**, *48*, 1663. (b) Seeman, N. C. *Annu. Rev. Biochem.* **2010**, *79*, 65. (c) Voigt, N. V.; Topping, T.; Rotaru, A.; Jacobsen, M. F.; Ravnsbaek, J. B.; Subramani, R.; Mamdouh, W.; Kjems, J.; Mokhir, A.; Besenbacher, F.; Gothelf, K. V. *Nat. Nanotechnol.* **2010**, *5*, 200.
- (5) (a) Wilner, O. I.; Weizmann, Y.; Gill, R.; Lioubashevski, O.; Freeman, R.; Willner, I. *Nat. Nanotechnol.* **2009**, *4*, 249. (b) Delebecque, C. J.; Lindner, A. B.; Silver, P. A.; Aldaye, F. A. *Science* **2011**, *333*, 470.
- (6) (a) Niemeyer, C. M.; Koehler, J.; Wuerdemann, C. *ChemBioChem* **2002**, *3*, 242. (b) Erkelenz, M.; Kuo, C. H.; Niemeyer, C. M. *J. Am. Chem. Soc.* **2011**, *133*, 16111.
- (7) Rothmund, P. W. K. *Nature* **2006**, *440*, 297.
- (8) Pinheiro, A. V.; Han, D.; Shih, W. M.; Yan, H. *Nat. Nanotechnol.* **2011**, *6*, 763.
- (9) Ke, Y.; Lindsay, S.; Chang, Y.; Liu, Y.; Yan, H. *Science* **2008**, *319*, 180.
- (10) Pathria, R. K. *Statistical Mechanics*, 2nd ed.; Butterworth-Heinemann: Woburn, MA, 1996; pp 459–464.
- (11) (a) Henzler, T.; Steudle, E. *J. Exp. Bot.* **2000**, *51*, 2053. (b) Stewart, P. S. *J. Bacteriol.* **2003**, *185*, 1485.
- (12) Bagchi, B. *Chem. Rev.* **2005**, *105*, 3197.
- (13) (a) Chung, Y.-H.; Xia, J.; Margulis, C. J. *J. Phys. Chem. B* **2007**, *111*, 13336. (b) Domínguez, L.; Sosa-Peinado, A.; Hansberg, W. *Arch. Biochem. Biophys.* **2010**, *500*, 82.
- (14) (a) Gorman, J.; Greene, E. C. *Nat. Struct. Mol. Biol.* **2008**, *15*, 768. (b) Jeltsch, A.; Pingoud, A. *Biochemistry* **1998**, *37*, 2160.
- (15) Mansson, M. O.; Siegbahn, N.; Mosbach, K. *Proc. Natl. Acad. Sci. U. S. A.* **1983**, *80*, 1487.
- (16) (a) Niemeyer, C. M. *Angew. Chem., Int. Ed. Engl.* **2010**, *49*, 1200. (b) Saccà, B.; Meyer, R.; Erkelenz, M.; Kiko, K.; Arndt, A.; Schroeder, H.; Rabe, K. S.; Niemeyer, C. M. *Angew. Chem., Int. Ed. Engl.* **2010**, *49*, 9378.